

Article

Aerodynamics Optimization of Multi-Blade Centrifugal Fan Based on Extreme Learning Machine Surrogate Model and Particle Swarm Optimization Algorithm

Fannian Meng¹, Liuji Wang¹, Wuyi Ming^{1,2,*} and Hongxiang Zhang¹

¹ Mechanical and Electrical Engineering Institute, Zhengzhou University of Light Industry, Zhengzhou 450002, China

² Guangdong Provincial Key Laboratory of Digital Manufacturing Equipment, Guangdong HUST Industrial Technology Research Institute, Dongguan 523808, China

* Correspondence: mingwuyi@zzuli.edu.cn

Abstract: The centrifugal fan is widely used in converting mechanical energy to aerodynamic energy. To improve the pressure of the multi-blade centrifugal fan used in an air purifier, an optimization process was proposed based on extreme learning machine (ELM) combined with particle swarm optimization (PSO). The blade definition position parameter and blade definition radian parameter were designed using the full-factor simulation experimental method. The steady numerical simulation of each experimental point was carried out using ANSYS CFX software. The total pressure of the multi-blade centrifugal fan was selected as the optimization response. The optimized ELM combined with the PSO algorithm considering the total pressure response value and the two multi-blade centrifugal fan parameters were built. The PSO algorithm was used to optimize the approximation blade profile to obtain the optimum parameters of the multi-blade centrifugal fan. The total pressure was improved from 140.6 Pa to 151 Pa through simulation experiment design and improved surrogate optimization. The method used in the article is meant for improving multi-blade centrifugal total pressure. The coupling optimization of impellers, volutes, and air intakes should be comprehensively considered to further improve the performance of centrifugal fans.

Keywords: multi-blade centrifugal fan; ELM surrogate model; PSO algorithm; optimization



Citation: Meng, F.; Wang, L.; Ming, W.; Zhang, H. Aerodynamics Optimization of Multi-Blade Centrifugal Fan Based on Extreme Learning Machine Surrogate Model and Particle Swarm Optimization Algorithm. *Metals* **2023**, *13*, 1222. <https://doi.org/10.3390/met13071222>

Academic Editors: João Manuel R. S. Tavares and Badis Haddag

Received: 3 May 2023

Revised: 8 June 2023

Accepted: 24 June 2023

Published: 2 July 2023



Copyright: © 2023 by the authors. Licensee MDPI, Basel, Switzerland. This article is an open access article distributed under the terms and conditions of the Creative Commons Attribution (CC BY) license (<https://creativecommons.org/licenses/by/4.0/>).

1. Introduction

The multi-blade centrifugal fan is widely used in household appliances such as air conditioners and range hoods; its advantages are its small size, large gas flow, low operating noise, and high pressure coefficient. It is sufficient to complete ventilation work while reducing the impact on the surrounding environment. With the development of industrial technology, multi-blade centrifugal fans are also widely used in industrial equipment such as air supply equipment for metallurgical boilers in metallurgical manufacturing plants and special element extraction equipment for reaction furnaces in nuclear power plants. Improving the performance of multi-blade centrifugal fans is of great significance for energy conservation and emission reduction.

In order to improve the performance of the centrifugal fan, scholars have conducted extensive research on multi-blade centrifugal fan optimization. Xu et al. [1] optimized the blade tip bionic groove parameters based on the flow control mechanism research of blade tip bionic grooves. Ye et al. [2] improved the multi-blade centrifugal fan performance by changing inlet structure parameters based on a bevel-cutting design method and computer simulation technology. Li et al. [3] studied the vortex characteristics of a multi-blade centrifugal fan near the volute outlet region. Wei et al. [4] researched the effect of clearance, the inclination angle, and the volute tongue on a multi-blade centrifugal fan's aerodynamic performance. Zhou et al. [5] adapted the SCT function parameterization method, RBF

surrogate model, and NSGA-II algorithm to optimize the multi-blade centrifugal fan blade parameters. Zhou et al. [6] optimized the multi-blade centrifugal fan total pressure efficiency and flow rate to improve the aerodynamic performance based on a modified Hicks–Henne function and Kriging agent model. Zhou et al. [7] proposed an optimal design method for multi-blade centrifugal fan using the Latin hypercube sampling design combined with the Kriging agent model. Alla et al. [8] optimized a squirrel cage on seven design parameters using the Latin hypercube sampling method and OpenFoam software (OpenFOAM foundation, open source, UK). Furthermore, Alla et al. [9] adapted the same method to optimize thirteen squirrel cage design parameters. Heo et al. [10] used the Latin hypercube sampling method, Kriging surrogate model, and genetic algorithm-II to optimize the impeller parameters. Le et al. [11] used ANSYS 15.0 software (ANSYS Inc., USA) to research the optimal operating conditions for the multi-blade centrifugal fan performance and flow characteristics. Kim et al. [12] used the numerical analysis and response surface optimization method to optimize the location of cutoff, radius of cutoff, width of the impeller, and flow coefficient. Table 1 shows the above optimization research on the multi-blade centrifugal fan, including optimization parameters and specific research methods.

Table 1. The optimization research on the multi-blade centrifugal fan.

Reference	Optimization Parameter	Method
Xu et al. [1]	Groove width, groove depth, groove center distance, groove number, different groove shapes	CFD simulation design method
Ye et al. [2]	Inner diameter, bevel-cutting blade	CFD technology, test
Li et al. [3]	Vortex characteristics	CFD technology
Wei et al. [4]	Clearance, the inclination angle, the volute tongue	CFD technology, test
Zhou et al. [5–7]	Multi-blade centrifugal fan blade airfoil parameter	<ol style="list-style-type: none"> 1. CST function parameterization 2. Latin hypercube sampling 3. RBF model 4. Non-dominant sorting genetic algorithm-II
Alla et al. [8,9]	Multi-blade centrifugal fan impeller and wheel parameter	<ol style="list-style-type: none"> 1. Latin hypercube sampling 2. Response surface approximation model 3. EGO approach
Heo et al. [10]	The scroll cut-off angle, the scroll diffuser expansion angle, the diameter ratio of the impeller, the blade exit angle	<ol style="list-style-type: none"> 1. Latin hypercube sampling 2. Kriging surrogate model 3. Algorithm-II
Le et al. [11]	Research operating condition on the centrifugal fan performance and flow characteristics, obtaining the topology optimization design	ANSYS software
Kim et al. [12]	Location of cutoff, radius of cutoff, width of impeller, flow coefficient	Numerical analysis, response surface optimization method

The main research methods for rotating machinery are based on CFD and the surrogate model. For example, among the above literature about multi-blade centrifugal fans, references [1–3,11] are based on CFD research and references [5–7,12] are based on CFD and surrogate model research.

For the rotating machinery of a centrifugal fan, the main research method is also based on the surrogate model. For example, Zhao et al. [13] adapted the reverse design method to optimize the geometric configuration of the centrifugal fan hood using the back-propagation neural networks surrogate model. Soheil et al. [14] used the Kriging surrogate model and MIGA algorithm to optimize the suction and shaft power of a vacuum cleaner centrifugal fan. Zhang et al. [15] used the DOE study, the RSM surrogate model, and the multi-objective genetic algorithm to optimize the fan's 13 design parameters. Lvo et al. [16] adapted the surrogate parameter optimization method to optimize the 3D vane shape. Jung et al. [17]

adapted the DOE method and the response surface methodology to optimize the diffuser of a small high-speed centrifugal fan. Zoran et al. [18] used the 3D parameterization method and the surrogate model to optimize the shape of fan vanes.

For the rotating machinery optimization of a compressor, the research method is also based on the CFD and surrogate model. Xu et al. [19] proposed the local remodeling surrogate model method used in the fluid analysis and structure optimization region of an impeller. Xu et al. [20] also optimized the impeller of a high-speed magnetic drive pump using the optimal Latin hypercube sampling method combined with the response surface methodology surrogate model. Tüchler et al. [21] introduced an aerodynamic shape optimization method for a micro-wave rotor turbine using the CFD model and hybrid algorithm. Furthermore, references [22,23] also optimized the compressor using the surrogate model.

Moreover, Zheng et al. [24] researched the internal flow characteristics of a centrifugal fan from changing edge curvatures of the impeller front disk using the CFD and test method. Engin, T. [25] researched the tip clearance effects for centrifugal fans using the CFD and test methods. References [26,27] optimized the centrifugal fan to obtain the minimize noise. Kruyt et al. [28] adapted the inverse method to design a centrifugal fan. Marian et al. [29] summarized the research method to improve operating efficiency and to reduce noise emissions for fans. Kudela et al. [30] summarized the surrogate model application advances for finite element computation.

The previously reported work mainly focuses on rotating machinery optimization using CFD technology, the surrogate model, and the intelligence algorithm. It can be proven that CFD technology combined with the surrogate model has good advantages in terms of rotating machinery optimization, this article adapted the frequently used method in optimizing the multi-blade centrifugal fan. In this article, the PSO algorithm is used to optimize the ELM surrogate model to improve the surrogate model fitting accuracy. The simulation experimental design method and improved surrogate optimization are used to improve the total pressure of the multi-blade centrifugal fan. The optimization has a wide range of areas and a large range of variables, which is conducive to achieving global optimization.

2. Optimization Problem Definition and Description

2.1. Optimization Object

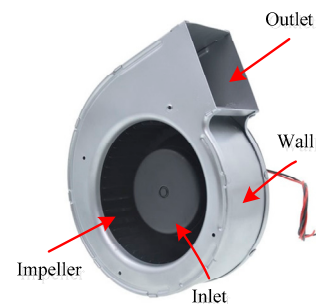
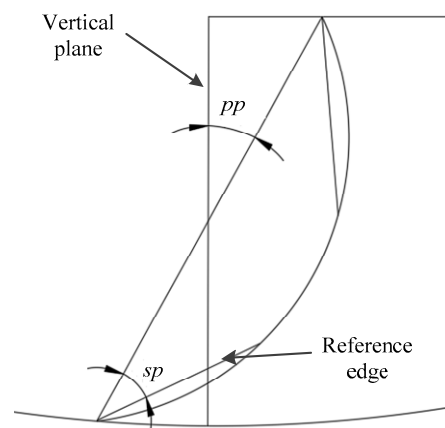
The research object is one particular type of multi-blade centrifugal fan, which is typically constructed with a built-in motor and is easy to disassemble. The structural parameters of this type of centrifugal fan are shown in Table 2, and its shape is shown in Figure 1.

Setting the blade length as 15 mm, width as 1 mm, and height as 43 mm, and using the plane perpendicular to the width of the blade and over the midpoint of the width as the reference plane (the reference plane is the same as the shape of the blade surface), it is necessary to ensure that the length of the reference line in each simulation model is equal.

The measurement criteria for different blade positions are different values for the included angle between the reference plane and the vertical plane (unit is defined as $^{\circ}$), and the measurement criteria for different blade shapes are different values for the included angle between the 5 mm side line at both ends of the reference line and the reference line (unit is also defined as $^{\circ}$). The blade profile position definition is shown in Figure 2, where each plane is shown from the top view.

Table 2. Structural parameters of the multi-blade centrifugal fan.

Structural Parameters	Value (mm)
Height	180
Width	61
Length	171
Diameter	133
Inlet diameter	110
Outlet parameter	59 × 71

**Figure 1.** Structural model of the multi-blade centrifugal fan.**Figure 2.** The blade profile position definition diagram.

2.2. Optimization Model

The air volume and total pressure are used to ensure the gas delivery for the multi-blade centrifugal fan. The total pressure (Tp) value is set as an optimization target; the multi-blade centrifugal fan position parameter (pp) and the shape parameter (sp) are optimization parameters. The multi-blade centrifugal fan optimization model is described as follows[5]:

$$\begin{aligned}
 &\text{find } x = (pp, sp) \\
 &\max \widehat{Tp}(x) \\
 &\text{s.t. } pp^{LB} \leq pp \leq pp^{UB} \\
 &\quad sp^{LB} \leq sp \leq sp^{UB}
 \end{aligned} \tag{1}$$

where pp is the position parameter for the blade, sp is the radian parameter for the blade, and \widehat{Tp} is the surrogate model approximate response value for total pressure, and this value is calculated using the ELM surrogate model optimized by the PSO algorithm.

2.3. Flowchart of Blade Parameter Optimization

Firstly, the pp and sp parameters are fully factorial simulation experimental design. Secondly, the optimal blade position parameters and shape parameters are obtained according to the process of Figure 3.

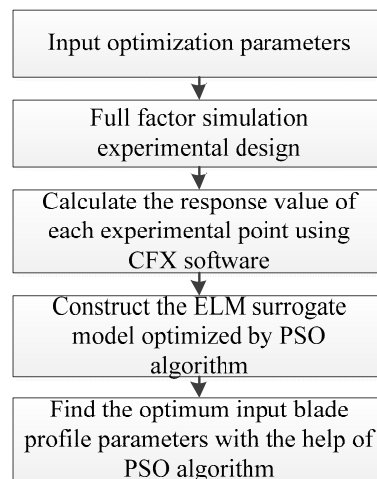


Figure 3. The optimization process flowchart.

3. The Surrogate Model and Optimization Algorithm

3.1. ELM Surrogate Model

Machine learning methods like neural networks are used in many fields [31–33]. Compared with the traditional neural networks, the ELM surrogate model has a faster learning speed and better generalization ability. The training model for the ELM method is shown in Figure 4.

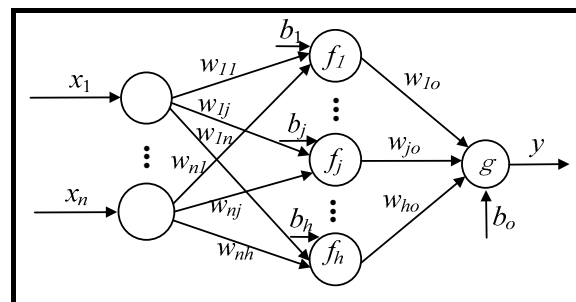


Figure 4. Extreme learning machine network architecture.

In Figure 4, n is the number of the input variables, h is the number of the hidden layer neurons, x_i is the input variable, $i = 1, 2, 3, \dots, n$, w_{ij} denotes the connection weights between the input variables and the hidden layer neurons j , w_{jo} denotes the connection weights between the hidden layer neurons j and the output layer, b_j denotes the threshold of the neurons in the hidden layer, $j = 1, 2, 3, \dots, h$, b_0 denotes the threshold of neurons in the output layer, $f_j(\cdot)$ denotes the activation function of the neurons in the hidden layer, and $g(\cdot)$ denotes the activation function of the neurons in the output layer.

Its mathematical model as follows [34]:

$$\begin{cases} y = g(b_0 + \sum_{j=1}^h w_{jo}v_j) \\ v_j = f_j(b_j + \sum_{i=1}^n w_{ij}x_i) \end{cases} \quad (2)$$

where v_j represents the output of a neuron j in the output layer.

If there are N valid samples, when the output threshold is equal to 0 and the output neuron activation function is a linear function, then Formula (2) can be rewritten as follows:

$$y = (w_o^T v)^T \quad (3)$$

where $y = [y(1), y(2), \dots, y(N)]^T$ is the network output vector, $w_o = [w_{1o}, w_{2o}, \dots, w_{ho}]^T$ is the output weight vector, and v is the output matrix of the hidden layer neurons, where the input weight and the threshold matrix w are generated randomly.

$$\left\{ \begin{array}{l} v = \begin{bmatrix} v_1(1) & v_1(2) & \cdots & v_1(N) \\ v_2(1) & v_2(2) & \cdots & v_2(N) \\ \vdots & \vdots & \cdots & \vdots \\ v_h(1) & v_h(2) & \cdots & v_h(N) \end{bmatrix} \\ w = \begin{bmatrix} b_1 & b_2 & \cdots & b_h \\ w_{11} & w_{12} & \cdots & w_{1h} \\ \vdots & \vdots & \cdots & \vdots \\ w_{n1} & w_{n2} & \cdots & w_{nh} \end{bmatrix} \end{array} \right. \quad (4)$$

The output weight vector is expressed as

$$w_o = v^* y_e \quad (5)$$

where v^* denotes the Moore–Penrose generalized inverse for output layer matrix v and $y_e = [y_e(1) \ y_e(2) \ \cdots \ y_e(N)]^T$ is the expected outputs. If there are $v \in R^{N \times h}$, $N \geq h$, and $\text{rank}(v) = h$, the Moore–Penrose generalized inverse v^* for v can be expressed as

$$v^* = (v^T v)^{-1} v^T \quad (6)$$

Formula (6) is introduced into Formula (5):

$$w_o = (v^T v)^{-1} v^T y_e \quad (7)$$

The activation function of the hidden layer used is the sigmoid function shown below:

$$f(a, b, x) = \frac{1}{1 + e^{-ax-b}} \quad (8)$$

Because the extreme learning machine avoids the disadvantages of traditional networks such as learning rate, termination conditions, and being easily trapped in a local optimum, this method can construct a surrogate model more effectively than other feed-forward neural networks. However, an extreme learning machine may need more hidden layer neurons than a traditional neural network, and it may lead to ill-conditioned problems because of randomly assigning input weights and thresholds. To solve this problem, particle swarm optimization (PSO) is used to optimize the ELM and apply it to the multi-blade centrifugal fan optimization process.

3.2. Particle Swarm Optimization

PSO was proposed by Eberhart and Kennedy in 1995 based on artificial life and evolutionary computing theory [35]. The basic idea is derived from the foraging behavior of birds. In PSO, the solution of each optimization problem is a bird in the search space, which is called a particle. Each particle has an initialization speed and position, and the fitness value is determined by the fitness function. Each particle is given a memory function to remember the best location to be searched. In addition, the speed of each particle determines the direction and distance of its flight so that the particle can search in the optimal solution space. In the iteration, the particle updates its speed and position by comparing fitness values and two extremes: the optimal solution found by the particle itself (individual extreme value) and the optimal solution currently found by the whole population (global extreme value):

$$v_i(t+1) = \omega v_i(t) + c_1 R_1 [R_i^b(t) - x_i(t)] + c_2 R_2 [R_g^b(t) - x_i(t)] \quad (9)$$

$$x_i(t+1) = x_i(t) + \phi v_i(t+1) \quad (10)$$

where t is the number of the iterations, $v_i(t)$ represents the speed of the t iteration for particle i , ω is the inertia weight, c_1, c_2 is the cognitive coefficient, R_1, R_2 is the uniformly distributed random number, $R_i^b(t)$ is the optimum position of individual history for particle i , $R_g^b(t)$ is the optimum position of group history, $x_i(t)$ is the position of the particle in the t iteration, and ϕ is a contraction factor used to keep the speed within a certain range.

As a random search and parallel optimization algorithm, the PSO algorithm has the characteristics of simplicity, robustness, easy realization, and fast convergence, and can find the global optimal solution of the problem with a relatively high probability.

3.3. Extreme Learning Machine Based on PSO

According to the basic principles of ELM, we can see that the input layer weight matrix w and the hidden layer threshold matrix b of ELM are generated randomly. Therefore, when the ELM model is fixed, the prediction error of ELM will be very large. PSO has good global optimization ability. PSO can find the optimal initial w and b for the ELM model, and then obtain the optimal ELM model. The main steps of the PSO-ELM algorithm are as follows:

1. Preprocessing of experimental data. The experimental data are divided into training sets and test sets, and then normalized.
2. The parameters of particle swarm optimization are transformed into ELM parameters, and then the input and output samples are sent to ELM for prediction and the fitness is calculated.
3. The individual and global extremums for all particles are calculated.
4. According to the formula of particle renewal speed and position, the particle velocity, position, and weight are updated.
5. When the number of iterations reaches the maximum number of iterations set or the fitness meets the requirements, the search is stopped; otherwise, the iterations are repeated until the condition of stopping iterations is reached.
6. The PSO-ELM model is completed. The particle position corresponding to the optimal individual is the optimal weights and thresholds of the ELM network, which are substituted into the ELM model.

The flow chart of the PSO-ELM algorithm is shown in Figure 5.

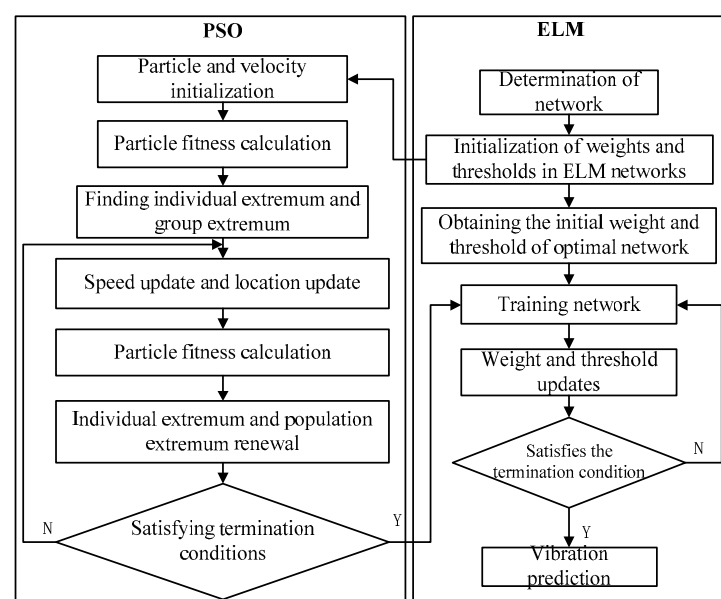


Figure 5. Algorithmic flow of PSO-ELM.

4. Concrete Optimization Process and Results

4.1. Optimization Structural Model

To ensure that the simulation results of the multi-blade centrifugal fan are consistent with the actual value, it is important to make the simulation model as close as possible to the actual working conditions. However, if the simulation model is too complex, the simulation time will be too long to bear. Therefore, it is necessary to simplify the simulation model of the multi-blade centrifugal fan appropriately. In addition, in combination with the requirements of the ANSYS CFX simulation, multiple boundaries need to be defined in the simulation model of the multi-blade centrifugal fan. Furthermore, to ensure that the simulation model meets the simulation requirements, it is essential to establish a standardized approach to follow during the simulation. The specific design principles for the simulation model are as follows: the bolt, nut, gasket, protective net, and other sealing mechanisms of the whole multi-blade centrifugal fan have the least impact on the simulation results during the simulation process and should be deleted from the simulation model. The fillets and grooves on the inner and outer shells of the multi-blade centrifugal fan have little influence on the simulation results and can be omitted. For some arc surfaces on the shell, the connecting arc between the upper shell and the impeller, the built-in motor chip, and the coil can be simplified with regular geometry.

4.2. CFX Simulation

The aerodynamics simulation involves meshing the inlet part, impeller, and volute. The grid division software used is ICEM. The generated grids are then checked using the Check-mesh function in ICEM software (ANSYS Inc., Canonsburg, PA, USA), and then the grids are optimized by the Smooth-Mesh-Globally function in ICEM software. The minimum angle of the grid is required to be greater than 14° to ensure grid quality. The impeller and volute simulation model that completes the grid division is shown in Figure 6.

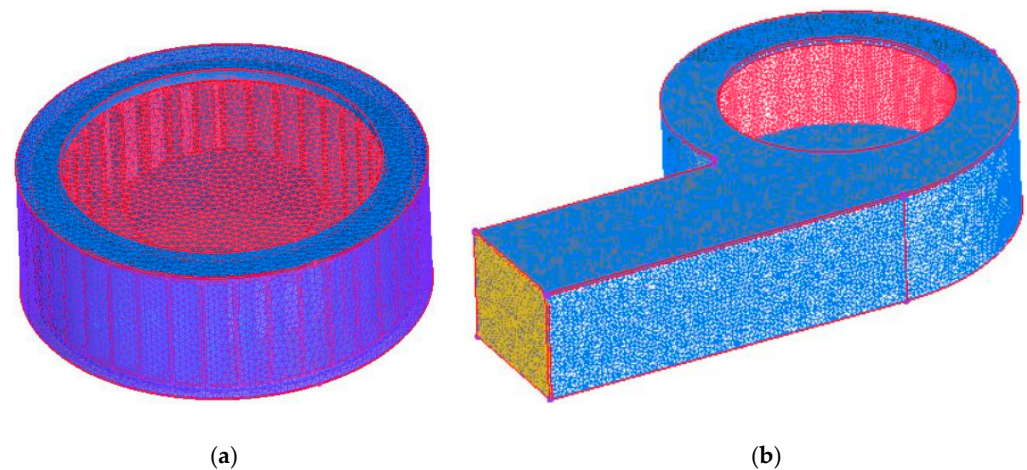


Figure 6. The generated grid for the multi-blade centrifugal fan. (a) Impeller, (b) volute.

In addition, in the working process of a multi-blade centrifugal fan, due to the fact that the number of blades is large, the blade distribution is dense, and the space between blades is short, the blade channel is narrow, so an internal secondary flow exists in the volute, forming a relatively complex three-dimensional asymmetric flow. For three-dimensional asymmetric flow, the calculation accuracy will be affected by the turbulence model used. Three-dimensional asymmetric flow often uses the Spalart–Allmaras, standard, and SST turbulence models. It is found that the standard model and SST model can better capture the vortex position and velocity gradient under the condition of small flow through existing research. In addition, due to the thickness of the blade and the fact that the standard model does not consider the wall shear force, there is an error between the numerical value obtained through the CFD simulation and the experimental value. Therefore, in the CFD

simulation process, the SST model is used as the turbulence model to improve the accuracy of the simulation.

The author used the same CFD simulation technology to simulate another type of centrifugal fan in reference [36], and it was verified that the CFD simulation results used in the article are in good agreement with the experimental results. In this article's CFD simulation, the same CFD simulation technology was used. Through comparative analysis, the CFD simulation technology used in this paper is reliable and can be used for the optimization analysis of multi-blade centrifugal fans.

4.3. Design of Simulation Experiment

Due to the substantial cost of simulation calculation, the optimized ELM surrogate model is introduced to replace the implicit relationship between the blade parameters and the total pressure responses for the multi-blade centrifugal fan, then the optimized ELM surrogate model is settled as the fitness function used in the PSO optimization process. The multi-blade centrifugal fan parameters pp and sp are in the design space. The ranges of the parameters pp and sp are set from 0° to 40° , there is full factor simulation experimental design for parameters pp and sp , the input parameters and response parameters are shown in Table 3, and the total pressure response values corresponding to each of the input parameters pp and sp are calculated using CFX software (ANSYS Inc., Canonsburg, PA, USA).

Table 3. Input parameter and response parameter settings.

Sequence	Position Parameter/ $^\circ$	Shape Parameter/ $^\circ$	Total Pressure/Pa
1	0	0	49.73
2	0	10	69.41
3	0	20	91.23
4	0	30	106.10
5	0	40	99.23
6	10	0	50.32
7	10	10	77.76
8	10	20	110.20
9	10	30	129.80
10	10	40	140.60
11	20	0	49.05
12	20	10	71.45
13	20	20	119.20
14	20	30	134.20
15	20	40	150.10
16	30	0	43.04
17	30	10	70.02
18	30	20	103.91
19	30	30	109.7
20	30	40	130.90
21	40	0	30.27
22	40	10	74.29
23	40	20	101.10
24	40	30	86.80
25	40	40	80.35

The simulation results table will be summarized based on the blade position. The blade position data and corresponding fan total pressure data for different blade shapes will be summarized. These summarized data will then be used to plot the corresponding images, as shown in Figure 7.

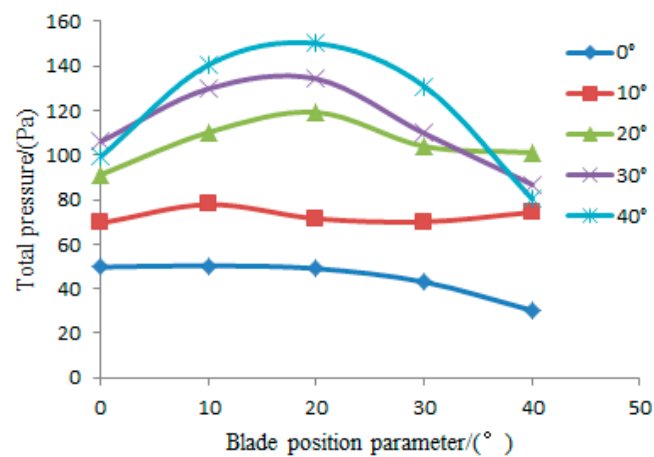


Figure 7. The relationship between the blade position parameters and total pressure.

As can be seen from the above figure, when the blade shape parameter is equal to 0° , the overall total pressure monotonically decreases with an increase in the blade position parameter. Furthermore, the decreasing slope of the blade increases with an increase in the blade position angle. When the blade shape angle ranges from 10° to 50° , the overall total pressure initially increases and then decreases as the blade position angle increases. Within the range of 20° to 40° for the blade shape angle, the maximum value of the overall wind total pressure is observed near the blade shape angle of 20° . It is also noteworthy that the total pressure of the multi-blade centrifugal fan increases as the blade angle increases at a constant blade position angle. The blade position parameters significantly affect the total pressure of a multi-blade centrifugal fan, mainly because the position of the blades is closely related to the airflow inside the impeller. Appropriate position parameters can reduce vortex loss and improve flow efficiency.

Figure 8 illustrates the relationship between blade shape parameters and the total pressure of a multi-blade centrifugal fan for different blade position parameters.

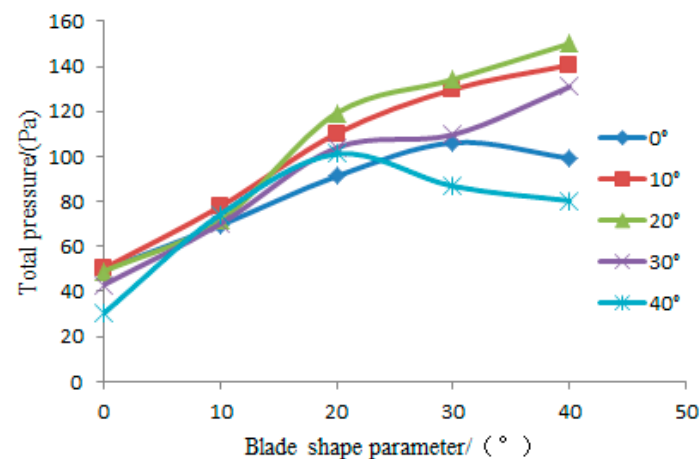


Figure 8. The relationship between the blade shape parameters and total pressure.

From Figure 8, it is evident that the total pressure increases monotonically as the blade shape angle increases within the range of 10° to 30° . When the blade position angles are between 0° and 40° , the total pressure initially increases and then decreases as the blade shape angle increases. When the blade position angle range is from 0° to 20° , the total pressure of the multi-blade centrifugal fan increases gradually for each corresponding blade shape, and when the blade position angle is from 20° to 40° , the total pressure gradually decreases for each blade shape angle. When the blade position angle is set to 20° , the total pressure of the multi-blade centrifugal fan corresponding to each blade shape angle is

generally greater than the total pressure corresponding to other blade shape angles. This provides further reference to increase the value of the shape for the multi-blade centrifugal fan and the total pressure required for subsequent designs.

To obtain the blade parameters pp and sp , corresponding to the maximum total pressure response value, the fitness function is needed in the optimization process of the PSO algorithm. Here, the PSO-ELM surrogate model is settled as a fitness function of the PSO optimization process, and the error index R^2 is used to evaluate the accuracy between the PSO-ELM and ELM methods. The coefficient R^2 is shown below:

$$R^2 = 1 - \frac{\sum_{i=1}^m (y_i - \hat{y}_i)^2}{\sum_{i=1}^m (y_i - \bar{y})^2} \tag{11}$$

where R^2 represents the global relative error of the surrogate model. m represents the number of test samples used to evaluate the accuracy of the surrogate model. y_i represents the true value and \hat{y}_i represents the predicted value through the surrogate model. \bar{y} represents the average value of all true values. The accuracy evaluation values for the R^2 coefficient between the PSO-ELM and ELM surrogate model are shown in Figure 9 and Table 4.

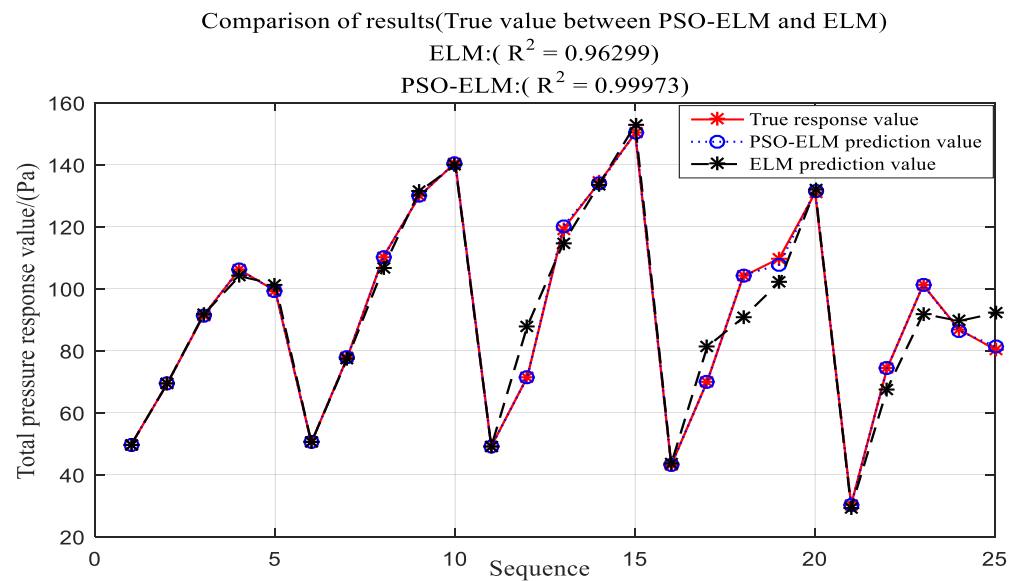


Figure 9. Fitting results evaluation between PSO-ELM and ELM method.

Table 4. Accuracy evaluation results for PSO-ELM and ELM.

Evaluation Index	PSO-ELM	ELM
R^2	0.99973	0.96299

The results in Figure 9 show that the PSO-ELM model is better than the ELM model in the fitting process. Moreover, the evaluation coefficient R^2 value is equal to 0.96299 for to the ELM model, and the R^2 value increases to 0.99973 for the PSO-ELM model.

The ELM model, Kriging model, and RBF model are discussed in the work [37] of Meng. In this study, the ELM model has the highest prediction accuracy compared with the Kriging model and RBF model, so the ELM model is used to predict multi-blade performance in the optimization process.

The article utilizes Matlab (MathWorks Inc., Natick, MA, USA) as the fitting software. In the prediction analysis conducted using Matlab, the ELM intelligent algorithm library

function is employed, and the software statement “[IW, B, LW, TF, TYPE] = elm_train (P_train, T_train, N, TF, TYPE);” is used, where “N” represents the number of hidden neurons, “TF” denotes the type of hidden layer activation function, and “TYPE” takes a value of 0 for classification and 1 for surrogate model prediction. After data training, the software statement ‘Tsim_2 = elm_predict (P_test, IW, B, LW, TF, TYPE);’ is used for proxy prediction.

To obtain the optimal blade parameters pp and sp , the PSO algorithm is employed. Figure 10 illustrates the optimization process with the PSO-ELM surrogate model set as the fitness function.

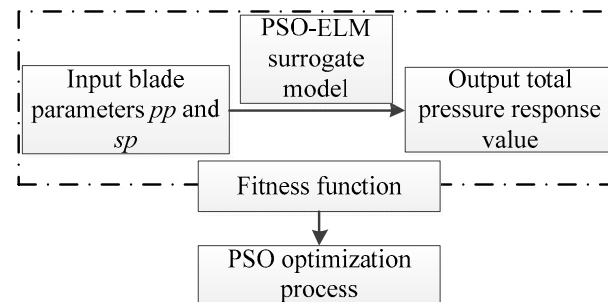


Figure 10. PSO optimization process.

Table 5 shows the optimization results for the maximum total pressure value optimized using the method shown in Figure 10.

Table 5. Total pressure value and blade parameters before and after optimization.

Centrifugal Fan	Blade Parameters [pp sp]/(°)	Total Pressure/(Pa)
Before optimization	(10.0, 40.0)	140.6
After optimization	(18.0, 39.0)	151

Table 5 illustrates the comparison of total pressure value before and after optimization. It is evident that the total pressure of the optimized fan has increased from 140.6 Pa to 150 Pa, indicating that the performance of the multi-blade centrifugal fan is superior to that of the original centrifugal fan.

5. Results and Discussion

Overall, with the increase in blade position parameters, the total pressure exhibits a trend of initially increasing and then decreasing. As the blade shape parameter increases, the overall total pressure shows an upward trend.

The method utilized in this article can enhance the total pressure of multi-blade centrifugal fans.

For future research on centrifugal fans, it is crucial to comprehensively consider the coupling optimization of impellers, volutes, and air intakes. This approach will lead to further improvements in the performance of centrifugal fans.

6. Conclusions

In this article, the PSO algorithm is used to improve the accuracy of the ELM model, and the PSO-ELM surrogate model is established, the PSO algorithm is used for optimization, and a blade profile optimization design process considering the aerodynamic performance of the multi-blade centrifugal fan is proposed.

- Using the CFD method to solve aerodynamic performance is complex and time-consuming. The PSO-ELM surrogate model set as the fitness function is used in the PSO optimization process. From the evaluation index R^2 , the R^2 value is equal to

0.99973 for the PSO-ELM model and the R^2 value is equal to 0.96299 for the ELM model; the accuracy of the PSO-ELM surrogate model has increased.

2. The total pressure is improved from 140.6 Pa to 151 Pa after optimization using simulation experiment design and the PSO algorithm.
3. This paper applied the modified ELM model to the optimal design of the multi-blade centrifugal fan and verifies the feasibility of coupling the modified ELM model and PSO algorithm to the blade parametric design. It provides new ideas for the optimal design of multi-blade centrifugal fans and other centrifugal fans. The entire optimization design has certain engineering use value.

Author Contributions: Conceptualization, F.M. and W.M.; methodology, F.M.; software, F.M.; validation, L.W., W.M. and H.Z.; formal analysis, H.Z.; investigation, W.M.; resources, H.Z.; data curation, H.Z.; writing—original draft preparation, L.W.; writing—review and editing, F.M.; supervision, W.M.; project administration, W.M.; funding acquisition, F.M. All authors have read and agreed to the published version of the manuscript.

Funding: This paper was supported by the key science and technology research project of Henan Province (No. 212102210071), and was also supported by the Local Innovative and Research Teams Project of the Guang-dong Pearl River Talents Program (No. 2017BT01G167).

Data Availability Statement: No new data were created or analyzed in this study. Data sharing is not applicable to this article.

Conflicts of Interest: The authors declare no conflict of interest.

References

1. Xu, Z.; Liu, X.; Liu, Y.; Qin, W.; Xi, G. Flow Control Mechanism of Blade Tip Bionic Grooves and Their Influence on Aerodynamic Performance and Noise of Multi-Blade Centrifugal Fan. *Energies* **2022**, *15*, 3431. [\[CrossRef\]](#)
2. Ye, J.; Liu, W.; Duan, P.; Huang, X.; Shao, J.; Zhang, Y. Investigation of the Performance and Flow Behaviors of the Multi-blade Centrifugal Fan Based on the Computer Simulation Technology. *Wirel. Pers. Commun.* **2018**, *103*, 563–574. [\[CrossRef\]](#)
3. Li, Z.; Ye, X.; Wei, Y. Investigation on Vortex Characteristics of a Multi-Blade Centrifugal Fan near Volute Outlet Region. *Processes* **2020**, *8*, 1240. [\[CrossRef\]](#)
4. Wei, Y.; Wang, J.; Xu, J.; Wang, Z.; Luo, J.; Yang, H.; Zhu, Z.; Zhang, W. Effects of Inclined Volute Tongue Structure on the Internal Complex Flow and Aerodynamic Performance of the Multi-Blade Centrifugal Fan. *J. Appl. Fluid Mech.* **2022**, *15*, 901–916. [\[CrossRef\]](#)
5. Zhou, S.; Yang, K.; Zhang, W.; Zhang, K.; Wang, C.; Jin, W. Optimization of Multi-Blade Centrifugal Fan Blade Design for Ventilation and Air-Conditioning System Based on Disturbance CST Function. *Appl. Sci.* **2021**, *11*, 7784. [\[CrossRef\]](#)
6. Zhou, S.; Zhou, H.; Yang, K.; Dong, H.; Gao, Z. Research on blade design method of multi-blade centrifugal fan for building efficient ventilation based on Hicks-Henne function. *Sustain. Energy Technol. Assess.* **2021**, *43*, 100971. [\[CrossRef\]](#)
7. Zhou, S.; Dong, H.; Zhang, K.; Zhou, H.; Jin, W.; Wang, C. Optimal design of multi-blade centrifugal fan based on partial coherence analysis. *Proc. Inst. Mech. Eng. Part C J. Mech. Eng. Sci.* **2022**, *236*, 894–907. [\[CrossRef\]](#)
8. Le Hocine, A.E.B.; Poncet, S.; Fellouah, H. CFD modeling and optimization by metamodels of a squirrel cage fan using OpenFoam and Dakota: Ventilation applications. *Build. Environ.* **2021**, *205*, 108145. [\[CrossRef\]](#)
9. Le Hocine, A.E.B.; Poncet, S.; Fellouah, H. Optimization of a double-intake squirrel cage fan using OpenFoam and metamodels. *Int. J. Heat Fluid Flow* **2023**, *101*, 109129. [\[CrossRef\]](#)
10. Heo, M.-W.; Kim, J.-H.; Seo, T.-W.; Kim, K.-Y. Aerodynamic and aeroacoustic optimization for design of a forward-curved blades centrifugal fan. *Proc. Inst. Mech. Eng. Part A J. Power Energy* **2016**, *230*, 154–174. [\[CrossRef\]](#)
11. Le, T.-L.; Nghia, T.T.; Thong, H.D.; Son, M.H.K. Numerical study of aerodynamic performance and flow characteristics of a centrifugal blower. *Int. J. Intell. Unmanned Syst.* **2022**. *ahead-of-print*. [\[CrossRef\]](#)
12. Kim, K.-Y.; Seo, S.-J. Application of Numerical Optimization Technique to Design of Forward-Curved Blades Centrifugal Fan. *JSME Int. J. Ser. B* **2006**, *49*, 152–158. [\[CrossRef\]](#)
13. Zhao, D.; You, X.-Y. Inverse design optimisation of a novel range hood based on intelligent algorithms and computational fluid dynamics simulations. *Adv. Powder Technol.* **2020**, *31*, 730–745. [\[CrossRef\]](#)
14. Almasi, S.; Ghorani, M.M.; Haghighi, M.H.S.; Mirghavami, S.M.; Riasi, A. Optimization of a vacuum cleaner fan suction and shaft power using Kriging surrogate model and MIGA. *Proc. Inst. Mech. Eng. Part A J. Power Energy* **2022**, *236*, 519–537. [\[CrossRef\]](#)
15. Zhang, J.; Zangeneh, M. Multi-Point, Multi-Objective Optimisation of Centrifugal Fans by 3D Inverse Design Method. *Int. J. Turbomachinery, Propuls. Power* **2023**, *8*, 8. [\[CrossRef\]](#)
16. Lvo, M.; Damir, V. 3D shape 3D shape optimization of fan vanes for multiple operating regimes subject to efficiency and noiserelated excellence criteria and constraints. *Eng. Appl. Comput. Fluid Mech.* **2016**, *10*, 209–277.

17. Jung, U.-H.; Kim, J.-H.; Kim, J.-H.; Park, C.-H.; Jun, S.-O.; Choi, Y.-S. Optimum design of diffuser in a small high-speed centrifugal fan using CFD & DOE. *J. Mech. Sci. Technol.* **2016**, *30*, 1171–1184. [[CrossRef](#)]
18. Zoran, M.; Damir, V.; Ivo, M. Multi-Regime Shape Optimization of Fan Vanes for Energy Conversion Efficiency using CFD, 3D Optical Scanning and Parameterization. *Eng. Appl. Comput. Fluid Mech.* **2014**, *8*, 407–421.
19. Xu, H.; Wei, W.; He, H.; Yang, X. Fluid Analysis and Structure Optimization of Impeller Based on Surrogate Model. *Comput. Model. Eng. Sci.* **2022**, *132*, 173–199. [[CrossRef](#)]
20. Xu, Z.; Kong, F.; Zhang, K.; Zhu, H.; Wang, J.; Qiu, N. Optimization of the impeller for hydraulic performance improvement of a high-speed magnetic drive pump. *Adv. Mech. Eng.* **2022**, *14*, 16878132221104576. [[CrossRef](#)]
21. Tuchler, S.; Copeland, C. Numerical Optimization of a Micro-wave Rotor Turbine Using a Quasi-two-dimensional CFD Model and a Hybrid Algorithm. *Shock Waves* **2021**, *31*, 271–300. [[CrossRef](#)]
22. Hosseinimaab, S.; Tousi, A. Optimizing the performance of a single-shaft micro gas turbine engine by modifying its centrifugal compressor design. *Energy Convers. Manag.* **2022**, *271*, 116245. [[CrossRef](#)]
23. Chen, J.; Wu, G. Kriging-assisted design optimization of the impeller geometry for an automotive torque converter. *Struct. Multidiscip. Optim.* **2018**, *57*, 2503–2514. [[CrossRef](#)]
24. Zheng, S.; Shao, Z.; Liu, J.; Chen, J.; Li, Y.; Chai, M. Flow characteristics of a centrifugal fan with optimized edge curvatures of an impeller front disk. *Proc. Inst. Mech. Eng. Part A J. Power Energy* **2023**. [[CrossRef](#)]
25. Engin, T. Study of tip clearance effects in centrifugal fans with unshrouded impellers using computational fluid dynamics. *Proc. Inst. Mech. Eng. Part A J. Power Energy* **2006**, *220*, 599–610. [[CrossRef](#)]
26. Jeon, W.-H.; Lee, D.-J.; Rhee, H. An Application of the Acoustic Similarity Law to the Numerical Analysis of Centrifugal Fan Noise. *JSME Int. J. Ser. C* **2004**, *47*, 845–851. [[CrossRef](#)]
27. Rebecca, S.; Martin, B. Validation of the Lattice Boltzmann Method for Simulation of Aerodynamics and Aeroacoustics in a Centrifugal Fan. *Acoustics* **2020**, *2*, 735–752.
28. Kruyt, N.P.; Westra, R.W. On the inverse problem of blade design for centrifugal pumps and fans. *Inverse Probl.* **2014**, *30*, 065003. [[CrossRef](#)]
29. Piwowarski, M.; Jakowski, D. Areas of Fan Research—A Review of the Literature in Terms of Improving Operating Efficiency and Reducing Noise Emissions. *Energies* **2023**, *16*, 1042. [[CrossRef](#)]
30. Kudela, J.; Matousek, R. Recent advances and applications of surrogate models for finite element method computations: A review. *Soft Comput.* **2022**, *26*, 13709–13733. [[CrossRef](#)]
31. Zhang, Z.; Qiu, W.; Zhang, G.; Liu, D.; Wang, P. Progress in applications of shockwave induced by short pulsed laser on surface processing. *Opt. Laser Technol.* **2023**, *157*, 108760. [[CrossRef](#)]
32. Ming, W.; Sun, P.; Zhang, Z.; Qiu, W.; Du, J.; Li, X.; Zhang, Y.; Zhang, G.; Liu, K.; Wang, Y.; et al. A systematic review of machine learning methods applied to fuel cells in performance evaluation, durability prediction, and application monitoring. *Int. J. Hydrogen Energy* **2023**, *48*, 5197–5228. [[CrossRef](#)]
33. Wang, P.; Zhang, Z.; Hao, B.; Wei, S.; Huang, Y.; Zhang, G. Investigation on heat transfer and ablation mechanism of CFRP by different laser scanning directions. *Compos. Part B Eng.* **2023**, *262*, 110827. [[CrossRef](#)]
34. Mustafa, A.; Ahmad, T.; Rana, H. Swarm-Based Extreme Learning Machine Models for Global Optimization. *Comput. Mater. Contin.* **2022**, *70*, 6339–6362.
35. Kennedy, J.; Eberhart, R. Particle swarm optimization. In Proceedings of the ICNN'95-International Conference on Neural Networks, Perth, WA, Australia, 27 November–1 December 1995; Volume 4, pp. 1942–1948.
36. Meng, F.; Zhang, Z.; Su, X.; Li, L. Centrifugal fan Blade Optimization Based on Kriging Surrogate model. *Chin. Hydraul. Pneum.* **2023**, *47*, 85–91.
37. Meng, F.; Gong, X.; Du, W.; Wang, L.; Zhao, F.; Li, L. Vibration performance prediction and reliability analysis for rolling bearing. *J. Vibroeng.* **2021**, *23*, 327–346. [[CrossRef](#)]

Disclaimer/Publisher's Note: The statements, opinions and data contained in all publications are solely those of the individual author(s) and contributor(s) and not of MDPI and/or the editor(s). MDPI and/or the editor(s) disclaim responsibility for any injury to people or property resulting from any ideas, methods, instructions or products referred to in the content.